PHYSICAL REVIEW D **79,** 054008 (2009)

$h_{1T}^{\perp}$ and quark orbital angular momentum

Jun She, Jiacai Zhu, and Bo-Qiang Ma*

School of Physics and State Key Laboratory of Nuclear Physics and Technology, Peking University, Beijing 100871, China

(Received 30 October 2008; revised manuscript received 2 January 2009; published 12 March 2009)

We calculate the pretzelosity distribution ($h_{1T}^{\perp}$), which is one of the eight leading twist transverse momentum dependent parton distributions (TMDs), in the light-cone formalism. We find that this quantity has a simple relation with the quark orbital angular momentum distribution, thus it may provide a new possibility to access the quark orbital angular momentum inside the nucleon. The pretzelosity distribution can manifest itself through the $\sin(3\phi_h - \phi_S)$ asymmetry in semi-inclusive deep inelastic scattering process. We calculate the $\sin(3\phi_h - \phi_S)$ asymmetry at HERMES, COMPASS, and JLab kinematics and present our prediction on different targets including the proton, deuteron, and neutron targets. Inclusion of transverse momentum cut in data analysis could significantly enhance the $\sin(3\phi_h - \phi_S)$ asymmetry for future measurements.

DOI: 10.1103/PhysRevD.79.054008 PACS numbers: 12.39.Ki, 13.60.Le, 13.85.Ni, 13.88.+e

I. INTRODUCTION

The nucleon is a composite system, so its spin not only comes from the intrinsic spins of the constituents, but also from the orbital angular momenta due to the relative motion of quarks and gluons. One of the main tasks of hadron physics is to quantitatively know the contribution from each component of the above items. However, on the theoretical side, there are disputes on how to define these quantities, and decomposing the contribution from spin and orbital angular momentum parts in experiments is also not clear yet.

Conventionally, it seems easy to start from the QCD Lagrangian and follow the Nöther's theorem, and to write the conserved angular momentum as

$$\begin{aligned}\vec{J}_{\mathrm{QCD}} &= \int d^3x\psi^\dagger \frac{\vec{\Sigma}}{2}\psi + \int d^3x\psi^\dagger \vec{x}\times(-i\nabla)\psi \\ &\quad + \int d^3x\vec{E}^a \times \vec{A}^a + \int d^3x E^{ai}\vec{x}\times\nabla A^{ai} \\ &\equiv \vec{S}_q + \vec{L}_q + \vec{S}_g + \vec{L}_g, \end{aligned} \tag{1}$$

in which the four terms are identified as the quark spin, quark orbital angular momentum, gluon spin, and gluon orbital angular momentum, respectively. This definition has been used in many references [1,2], and it is naturally considered as the generator of the space rotation. In Ref. [2], the matrix elements of this defined orbital angular momentum operator in the light-cone representation were calculated, and the results satisfy the conservation of the z projection of angular momentum:

$$J^z = \sum_{i=1}^{n} s_i^z + \sum_{j=1}^{n-1} l_j^z. \tag{2}$$

But a problem is that except for the quark spin term, the other three terms are gauge dependent, thus they have obscure physical meanings in common situations.

By considering this, Ji suggested a gauge-invariant expression [3]:

$$\begin{aligned}\vec{J}_{\mathrm{QCD}} &= \int d^3x\psi^\dagger \frac{\vec{\Sigma}}{2}\psi + \int d^3x\psi^\dagger \vec{x}\times(-i\vec{D})\psi \\ &\quad + \int d^3x\vec{x}\times(\vec{E}\times\vec{B}) \\ &\equiv \vec{S}_q + \vec{L}_q + \vec{J}_g, \end{aligned} \tag{3}$$

where $\vec{D} = \nabla - ig\vec{A}$ is the covariant derivative. As pointed in Ref. [3], this can be experimentally accessed in the deep virtual Compton scattering (DVCS) process, where the total angular momentum $\vec{J}_q \equiv \vec{S}_q + \vec{L}_q$ can be measured, and HERMES Collaboration has reported their experimental progresses in recent years [4]. But in this definition, unlike the quark case, there exists no gauge-invariant decomposition of spin and orbital contributions for the gluon angular momentum $\vec{J}_g$. However, de Téramond and Brodsky showed recently [5] that under the framework of light-front QCD, there is a separation of the dynamics of quark and gluon binding from the kinematics of constituent spin and internal orbital angular momentum. More seriously, the assumed quark orbital angular momentum operator does not obey the angular momentum algebra $\vec{J}\times\vec{J} = i\vec{J}$, and there is an interaction term involving also gluons. So it is a question whether such a defined and measured quantity can be viewed as the quark orbital angular momentum.

Trying to reconcile the gauge invariance and the angular momentum algebra, Chen *et al.* proposed a new form of spin sum [6] by adding a surface term $\int d^3x\nabla\cdot[\vec{E}^a(\vec{A}^a_{\mathrm{pure}}\times\vec{x})]$, which vanishes after integration over the

*mabq@phy.pku.edu.cn

space,

$$\vec{J}_{\rm QCD} = \int d^3x\psi^\dagger \frac{\vec{\Sigma}}{2}\psi + \int d^3x\psi^\dagger \vec{x}\times(-i\vec{D}_{\rm pure})\psi + \int d^3x\vec{E}^a \times \vec{A}^a_{\rm phys} + \int d^3x E^{ai}\vec{x}\times\nabla A^{ai}_{\rm phys} \equiv \vec{S}_q + \vec{L}_q + \vec{S}_g + \vec{L}_g, \quad (4)$$

where $\vec{D}_{\rm pure} = \nabla - ig\vec{A}_{\rm pure}$, and $\vec{A}_{\rm pure}$ is the pure gauge component of $\vec{A}$, satisfying $\vec{D}_{\rm pure}\times\vec{A}_{\rm pure} = 0$. $\vec{A}$ can be decomposed as $\vec{A} = \vec{A}_{\rm pure} + \vec{A}_{\rm phys}$. In this definition, all terms are gauge invariant and obey the angular momentum algebra. But there is a practical problem of lacking a clear way to measure orbital angular momentum defined so far.

If we disregard the disputes on the definition, we can define various quantities under each frame of definition and investigate their properties. In Ref. [7], the first definition mentioned above was used and a quantity that represents the quark orbital angular momentum in the light-cone formalism was obtained. It was shown that the quark orbital angular momentum equals the difference between the helicity and transversity, but it was not clear how to measure this quantity directly at that time. In Ref. [8], Avakian *et al.* used the bag model and the spectator model to deduce the result that the difference of helicity and transversity is (a transverse moment of) the so-called pretzelosity, a new quantity which is one of the leading twist parton distributions. Later in Ref. [9], Pasquini *et al.* confirmed this statement but using the light-cone constituent quark model. Conventionally, the difference of helicity and transversity is viewed as the relativistic effects in the nucleon, so in Refs. [8,9], pretzelosity is considered as the measurement of the relativistic effects in the nucleon. In this paper, we calculate the pretzelosity distribution in the light-cone SU(6) quark-diquark model and reconfirm the conclusion as that in Refs. [8,9]. So combining with the result already obtained in Ref. [7], we suggest that pretzelosity might open a new way to access the quark orbital angular momentum. Of course we should remember that our definition and conclusion are based on the light-cone gauge in the infinite momentum frame (IMF), or equivalently, $A^+ = 0$ gauge in the light-cone formalism [10,11], which is the conventional language for describing parton distributions inside the nucleon. The advantages of using light-cone formalism to describe the quark orbital angular moment have been also stressed in Refs. [2,5].

II. TMDS AND PRETZELOSITY

Pretzelosity, usually denoted as $h_{1T}^\perp$, is one of the eight leading twist transverse dependent parton distributions (TMDs). Up to the leading twist, the decomposition of the quark-quark correlator reads [12,13]

$$\Phi(x,\boldsymbol{p}_\perp) = \frac{1}{2}\Big\{f_1\not{n}_+ - f_{1T}^\perp\frac{\epsilon_\perp^{ij}p_\perp^i S_\perp^j}{M_N}\not{n}_+ + \Big(S_\parallel g_{1L} + \frac{\boldsymbol{p}_\perp\cdot\boldsymbol{S}_\perp}{M_N}g_{1T}\Big)\gamma_5\not{n}_+ + h_{1T}\frac{[\not{S}_\perp,\not{n}_+]\gamma_5}{2} + \Big(S_\parallel h_{1L}^\perp + \frac{\boldsymbol{p}_\perp\cdot\boldsymbol{S}_\perp}{M_N}h_{1T}^\perp\Big)\times\frac{[\not{p}_\perp,\not{n}_+]\gamma_5}{2M_N} + ih_1^\perp\frac{[\not{p}_\perp,\not{n}_+]}{2M_N}\Big\}. \quad (5)$$

Using the abbreviation $\Phi^{[\Gamma]} = {\rm Tr}(\Phi\Gamma)/2$, we can get the traces of the correlator [12,13]

$$\Phi^{[\gamma^+]} = f_1 - S_\perp^j\frac{\epsilon_\perp^{ij}p_\perp^i}{M_N}f_{1T}^\perp, \quad (6)$$

$$\Phi^{[\gamma^+\gamma_5]} = S_\parallel g_{1L} + \frac{\boldsymbol{p}_\perp\cdot\boldsymbol{S}_\perp}{M_N}g_{1T}, \quad (7)$$

$$\Phi^{[i\sigma^{i+}\gamma_5]} = S_\perp^i h_1 + S_\parallel\frac{p_\perp^i}{M_N}h_{1L}^\perp + S_\perp^j\frac{2p_\perp^i p_\perp^j - p_\perp^2\delta_\perp^{ij}}{2M_N^2}h_{1T}^\perp - \frac{\epsilon_\perp^{ij}p_\perp^j}{M_N}h_1^\perp. \quad (8)$$

Working in the light-cone gauge, we have [12,14]

$$\Phi^{[\Gamma]} = \int\frac{d\xi^- d^2\boldsymbol{\xi}_\perp}{16\pi^3}e^{i(xP^+\xi^- - \boldsymbol{p}_\perp\cdot\boldsymbol{\xi}_\perp)} \times\langle PS|\bar\psi(0)\Gamma\psi(0,\xi^-,\xi_\perp)|PS\rangle. \quad (9)$$

The pretzelosity distribution can be worked out by

$$\frac{p_\perp^x p_\perp^y}{M_N^2}h_{1T}^\perp(x,p_\perp^2) = \int\frac{d\xi^- d^2\boldsymbol{\xi}_\perp}{16\pi^3}e^{i(xP^+\xi^- - \boldsymbol{p}_\perp\cdot\boldsymbol{\xi}_\perp)} \times\langle PS^y|\bar\psi(0)i\sigma^{1+}\gamma_5\psi(0,\xi^-,\xi_\perp)|PS^y\rangle, \quad (10)$$

where $|PS^y\rangle$ denotes the hadronic state with a polarization in y direction.

Pretzelosity is chirally odd, so it must couple with a chirally odd partner in the semi-inclusive deep inelastic scattering (SIDIS) process (see Sec. V). It is usually considered as a measure of the relativistic effects in the nucleon, and a detailed discussion on its property can be found in Ref. [8].

III. PRETZELOSITY IN THE LIGHT-CONE SU(6) QUARK-DIQUARK MODEL

The matrix element shown in Eq. (10) cannot be solved strictly since a proton state contains the nonperturbative information. Conventionally, this state can be expanded in a series of light-cone Fock states with coefficients, i.e., the light-cone wave functions, and all the wave functions contain the full information of the nucleon. In principle, there

is an infinite number of wave functions and the wave functions cannot be calculated perturbatively. However, this expansion can be truncated so that only the Fock states with a few partons necessary for calculation are left, and the finite number of wave functions can be parametrized by experiments or certain models. In this paper, we use the light-cone SU(6) quark-diquark model [15], in which the proton state is constructed by a valence quark and a spectator diquark. The advantage of this model is that some of the gluon and quark effects in the spectator can be effectively described by the diquark with a few parameters. However, as only valence quark distributions can be directly calculated in this model, one must use other information to take into account contributions from sea and gluon distributions.

Any hadron state can be expanded in terms of a complete set of Fock states at equal "light-cone time" [10,11]

$$|H\rangle = \sum_{n,\lambda_i} \int [dx][d^2\boldsymbol{k}_\perp] \psi_n(x_i, \boldsymbol{k}_{\perp i}, \lambda_i) \prod_q \frac{u(x_i P^+, x_i \boldsymbol{P}_\perp + \boldsymbol{k}_{\perp i}, \lambda_i)}{\sqrt{x_i}} \prod_g \frac{\boldsymbol{\epsilon}(x_i P^+, x_i \boldsymbol{P}_\perp + \boldsymbol{k}_{\perp i}, \lambda_i)}{\sqrt{x_i}} |n\rangle, \tag{11}$$

with the normalization condition

$$\sum_{n,\lambda_i} \int [dx][d^2\boldsymbol{k}_\perp] |\psi_n(x_i, \boldsymbol{k}_{\perp i}, \lambda_i)|^2 = 1, \tag{12}$$

and the integral over the phase space is

$$\begin{aligned} [dx] &= \delta\Big(1 - \sum_{i=1}^{n} x_i\Big) \prod_{i=1}^{n} dx_i, \\ [d^2\boldsymbol{k}_\perp] &= 16\pi^3 \delta^2\Big(\sum_{i=1}^{n} \boldsymbol{k}_{\perp i}\Big) \prod_{i=1}^{n} (d^2\boldsymbol{k}_{\perp i}/16\pi^3). \end{aligned} \tag{13}$$

In the SU(6) quark-diquark model, the proton state with a spin component $S_z = \pm\frac{1}{2}$ in the instant form can be written as

$$\begin{aligned} |p^\uparrow\rangle = \tfrac{1}{3}\sin\theta\varphi_V[(ud)^0 u^\uparrow - \sqrt{2}(ud)^1 u^\downarrow - \sqrt{2}(uu)^0 d^\uparrow \\ + 2(uu)^1 d^\downarrow]) + \cos\theta\varphi_S (ud)^S u^\uparrow, \end{aligned} \tag{14}$$

$$\begin{aligned} |p^\downarrow\rangle = -\tfrac{1}{3}\sin\theta\varphi_V[(ud)^0 u^\downarrow - \sqrt{2}(ud)^{-1} u^\uparrow - \sqrt{2}(uu)^0 d^\downarrow \\ + 2(uu)^{-1} d^\uparrow] + \cos\theta\varphi_S (ud)^S u^\downarrow, \end{aligned} \tag{15}$$

where θ is the mixing angle that breaks the SU(6) symmetry when $\theta \neq \pi/4$. More explicitly, we write the Fock expansion in a diquark model as

$$\begin{aligned} |PS^\uparrow\rangle = \sum_j \frac{1}{16\pi^3} \int \frac{dx_q dx_D}{\sqrt{x_q x_D}} \int d^2\boldsymbol{k}_{q\perp} d^2\boldsymbol{k}_{D\perp}, \\ \delta(1 - x_q - x_D)\delta^2(\boldsymbol{k}_{q\perp} + \boldsymbol{k}_{D\perp}) \psi(x_j, \boldsymbol{k}_{j\perp}, \lambda_i) a_j^\dagger b_j^\dagger |0\rangle, \end{aligned} \tag{16}$$

where the wave functions can be extracted from Eq. (14). The negative helicity state can be written in the same way.

Notice that now we are working in the instant frame, and we need to transform to the light-cone frame. The connection between the two frames is through a Melosh-Wigner rotation [16,17]. For a spin-$\frac{1}{2}$ particle, we use q_T and q_F to denote the instant and light-cone spinors, respectively, and the Melosh-Wigner rotation is known to be [17]

$$\begin{pmatrix} q_F^\uparrow \\ q_F^\downarrow \end{pmatrix} = \omega \begin{pmatrix} k^+ + m & -k^R \\ k^L & k^+ + m \end{pmatrix} \begin{pmatrix} q_T^\uparrow \\ q_T^\downarrow \end{pmatrix} \equiv \boldsymbol{M}^{1/2} \begin{pmatrix} q_T^\uparrow \\ q_T^\downarrow \end{pmatrix}, \tag{17}$$

where $k^{R,L} = k_1 \pm ik_2$, $\omega = [(x\mathcal{M}_D + m_q)^2 + p_\perp^2]^{-1/2}$ with $\mathcal{M}_D^2 = \frac{m_q^2 + p_\perp^2}{x} + \frac{m_D^2 + p_\perp^2}{1-x}$, m_q and m_D are mass parameters for the quark and diquark, and $\boldsymbol{M}^{1/2}$ denotes the Melosh-Wigner rotation matrix with the superscript referring to the spin of the particle. For the spin-0 scalar diquark, there is no such transformation. For the spin-1 vector diquark, the transformation is represented by a 3×3 matrix $\boldsymbol{M}^1$, whose explicit expression can also be found in Ref. [18]. In practice, we will not use the explicit form, for it does not appear in the final expression for the spectator debris due to the unitary property $\boldsymbol{M}^{1\dagger}\boldsymbol{M}^1 = 1$.

Using Eqs. (9), (11), (16), and (17), we deduce the formula for calculating the trace of the correlator:

$$\phi^{[\Gamma]} = \sum_{j,\lambda,\lambda',\lambda_D} \frac{1}{32\pi^3} \frac{1}{xP^+} \psi_j^*(x, \boldsymbol{p}_\perp, \lambda; 1-x, -\boldsymbol{p}_\perp, \lambda_D) \psi_j(x, \boldsymbol{p}_\perp, \lambda'; 1-x, -\boldsymbol{p}_\perp, \lambda_D) \bar{u}(xP^+, \boldsymbol{p}_\perp, \lambda) \Gamma u(xP^+, \boldsymbol{p}_\perp, \lambda'). \tag{18}$$

We substitute $i\sigma^{1+}\gamma_5$ for Γ and notice that $|P^y\rangle = \frac{1}{\sqrt{2}}(|P^\uparrow\rangle + i|P^\downarrow\rangle)$, after a careful calculation, we get the result for pretzelosity (the superscript v denotes that it is valid only for valence quarks):

$$h_{1T}^{\perp(uv)}(x, \boldsymbol{p}_\perp) = -\frac{1}{16\pi^3} \times \left(\frac{1}{9}\sin^2\theta\varphi_V^2 W_V - \cos^2\theta\varphi_S^2 W_S\right),$$
$$h_{1T}^{\perp(dv)}(x, \boldsymbol{p}_\perp) = -\frac{1}{8\pi^3} \times \frac{1}{9}\sin^2\theta\varphi_V^2 W_V, \tag{19}$$

with the Melosh-Wigner rotation factor $W_D(D = V, S)$ given by

$$W_D(x, \boldsymbol{p}_\perp) = -\frac{2M_N^2}{(x\mathcal{M}_D + m_q)^2 + p_\perp^2}, \tag{20}$$

which agrees with the result in Ref. [9], in which a three quark model was used. $\varphi_V(\varphi_S)$ are the wave functions in the momentum space for the vector (scalar) diquark, which can be parametrized by the Brodsky-Huang-Lepage (BHL) prescription [10,19]:

$$\varphi_D(x, \boldsymbol{p}_\perp) = A_D \exp\left\{-\frac{1}{8\alpha_D^2}\left[\frac{m_q^2 + p_\perp^2}{x} + \frac{m_D^2 + p_\perp^2}{1-x}\right]\right\}, \tag{21}$$

whose normalization should be consistent with Eq. (12). The parameters such as α_D, the quark mass m_q, and the diquark mass m_D can be found in Ref. [15], and we list them in Table I. In the same way, the unpolarized distributions can be derived [15]

$$f_1^{(uv)}(x, \boldsymbol{p}_\perp) = \frac{1}{16\pi^3} \times \left(\frac{1}{3}\sin^2\theta\varphi_V^2 + \cos^2\theta\varphi_S^2\right),$$
$$f_1^{(dv)}(x, \boldsymbol{p}_\perp) = \frac{1}{8\pi^3} \times \frac{1}{3}\sin^2\theta\varphi_V^2. \tag{22}$$

Using above formulas, we can calculate pretzelosity and the unpolarized distribution function independently, but this model calculation strongly depends on the choice of the wave function. The BHL form we use exhibits the sharp falloff at both the large and small x region, but the consequent result for the distribution functions might be inconsistent with the realistic situation. For example, the CTEQ6 extraction shows a divergence tendency at $x \to 0$, rather than 0 as Eq. (22) indicates.

In order to make our result more close to the realistic situation, we could adopt another prescription based on the results of our model. This can be done by combining Eqs. (19) and (22), then we get the relation between the unpolarized and pretzelosity distributions:

$$h_{1T}^{\perp(uv)}(x, \boldsymbol{p}_\perp) = [f_1^{(uv)}(x, \boldsymbol{p}_\perp) - \tfrac{1}{2}f_1^{(dv)}(x,)\boldsymbol{p}_\perp]W_S(x, \boldsymbol{p}_\perp) - \tfrac{1}{6}f_1^{(dv)}(x, \boldsymbol{p}_\perp)W_V(x, \boldsymbol{p}_\perp),$$
$$h_{1T}^{\perp(dv)}(x, \boldsymbol{p}_\perp) = -\tfrac{1}{3}f_1^{(dv)}(x, \boldsymbol{p}_\perp)W_V(x, \boldsymbol{p}_\perp). \tag{23}$$

TABLE I. Parameters.

α_D (MeV)	m_q (MeV)	m_S (MeV)	m_V (MeV)
330	330	600	800

Now, we will use the phenomenological extraction of the unpolarized distribution functions as an input to calculate the pretzelosity distribution. For example, we will use the CTEQ6L [20] parametrization to get $f_1(x)$, which have been well tested and constrained by many experiments. And then by combining with some assumed transverse momentum $\boldsymbol{p}_\perp$ factor one can get phenomenological $f_1(x, \boldsymbol{p}_\perp)$ as input to calculate the pretzelosity distribution $h_{1T}^\perp(x, \boldsymbol{p}_\perp)$.

Here we need to make some comments on Eq. (23). The left-hand side of the equation is a chiral-odd function, which does not have gluon counterparts. But the right-hand side is a linear combination of two chiral-even functions, which have gluon counterparts. So the two sides have different evolutions, which means that the relation cannot be held exactly at any scale. This paradox originates from the fact that the model we use is a no-gluon model, which was pointed out in Ref. [8]. Nevertheless, we can comprehend this relation from two aspects. First, we assume that Eq. (23) is valid at an initial scale. Second, the evolution effect for pretzelosity appearing on the left is partially (not all) contained in the unpolarized distribution. So we conclude that Eq. (23) could be approximately satisfied and useful for estimating pretzelosity, but we must be careful that the valid scale should not be too large.

The two approaches to calculate the pretzelosity distribution may lead to different results. We denote the former approach, i.e., the model calculation with wave function as input, as approach 1, and the latter one, i.e., with phenomenological parametrization of $f_1(x, \boldsymbol{p}_\perp)$ as input, as approach 2. Here we should emphasize again that we have used a "valence model," and we can only directly calculate valence quark distributions in principle. In approach 1, for both pretzelosity and unpolarized distribution, only the contribution from valence quarks can be considered due to a model calculation. In approach 2, the prescription for pretzelosity is the same as that in approach 1, but for unpolarized distribution, the phenomenological parametrization can provide us with the information on sea quarks so that we can take into account the sea contributions for the unpolarized processes. In this paper, we will use both approaches to obtain distribution functions and give predictions separately. Numerical results will be presented in Sec. V.

IV. PRETZELOSITY AND ORBITAL ANGULAR MOMENTUM

The effect of Melosh-Wigner rotation is also important in other leading twist distribution functions such as the helicity and transversity distributions, which have been extensively discussed in light-cone formalism in Refs. [15,21]. We find that all the distributions have similar form as Eq. (23) shows, but with different Melosh-Wigner rotation factors. The rotation factors for the helicity and transversity distributions are $\frac{(x\mathcal{M}_D+m_q)^2-p_\perp^2}{(x\mathcal{M}_D+m_q)^2+p_\perp^2}$ [15,17] and

$\frac{(x\mathcal{M}_D+m_q)^2}{(x\mathcal{M}_D+m_q)^2+p_\perp^2}$ [21], respectively. Note the simple relation

$$\frac{(x\mathcal{M}_D+m_q)^2-p_\perp^2}{(x\mathcal{M}_D+m_q)^2+p_\perp^2}-\frac{(x\mathcal{M}_D+m_q)^2}{(x\mathcal{M}_D+m_q)^2+p_\perp^2}=\frac{p_\perp^2}{2M_N^2}W_D(x,\boldsymbol{p}_\perp), \tag{24}$$

so we can immediately yield the equation

$$h_{1T}^{(1)qv}(x,\boldsymbol{p}_\perp)\equiv\frac{p_\perp^2}{2M_N^2}h_{1T}^{\perp qv}(x,\boldsymbol{p}_\perp)=g_1^{qv}(x,\boldsymbol{p}_\perp)-h_1^{qv}(x,\boldsymbol{p}_\perp), \tag{25}$$

where g_1 and h_1 denote the helicity and transversity distributions, respectively. This relation has already been obtained in Ref. [8] with a bag model and a spectator model, and also in Ref. [9] with a three-quark model. But in Ref. [22], this relation is not fully satisfied in a spectator model where the axial-vector coupling will spoil the relation. We think that this issue needs further discussing.

Now, we should point out that the Melosh-Wigner rotation factor for $h_{1T}^{\perp(1)qv}(x,\boldsymbol{p}_\perp^2)$ is $\frac{-p^2}{(x\mathcal{M}_D+m_q)^2+p_\perp^2}$, which is nothing else but the rotation factor $M_L(x,\boldsymbol{p}_\perp)$ with a minus sign introduced in Ref. [7]. More importantly, it is the rotation factor for the quark orbital angular momentum indicated in Ref. [7], so we see that there is a simple relation between the pretzelosity and the quark orbital angular momentum

$$L^{qv}(x,\boldsymbol{p}_\perp)=-h_{1T}^{\perp(1)qv}(x,\boldsymbol{p}_\perp)=h_1^{qv}(x,\boldsymbol{p}_\perp)-g_1^{qv}(x,\boldsymbol{p}_\perp), \tag{26}$$

or at the integration level

$$L^{qv}(x)=\int d^2\boldsymbol{p}_\perp L^{qv}(x,\boldsymbol{p}_\perp)=-h_{1T}^{\perp(1)qv}(x)=h_1^{qv}(x)-g_1^{qv}(x). \tag{27}$$

We should mention that the orbital angular momentum we denote here is under the definition that the quark orbital angular momentum operator is $\vec{x}\times(-i\nabla)$, and the gauge we choose is $A^+=0$.

V. PREDICTIONS ON THE $\sin(3\phi_h-\phi_S)$ ASYMMETRY AT HERMES, COMPASS, AND JLAB KINEMATICS

As we pointed out before the pretzelosity has a simple relation with the quark orbital angular momentum, thus a measurement of pretzelosity may reveal the information on the quark orbital angular momentum. Fortunately, the pretzelosity distribution can be measured through $\sin(3\phi_h-\phi_S)$ asymmetry in the SIDIS process [23,24], where the cross section can be written as

$$\frac{d^6\sigma_{UT}}{dxdyd\phi_S dzd^2\boldsymbol{P}_{h\perp}}=\frac{2\alpha^2}{sxy^2}\left\{\left(1-y+\frac{1}{2}y^2\right)F_{UU}+S_\perp\sin(3\phi_h-\phi_S)(1-y)F_{UT}^{\sin(3\phi_h-\phi_S)}+\text{other structure functions}\right\}, \tag{28}$$

with

$$F_{UU}=\mathcal{F}[f_1D_1], \tag{29}$$

$$F_{UT}^{\sin(3\phi_h-\phi_S)}=\mathcal{F}\left[\frac{2(\hat{\boldsymbol{h}}\cdot\boldsymbol{p}_\perp)(\boldsymbol{p}_\perp\cdot\boldsymbol{k}_\perp)+\boldsymbol{p}_\perp^2(\hat{\boldsymbol{h}}\cdot\boldsymbol{k}_\perp)-4(\hat{\boldsymbol{h}}\cdot\boldsymbol{p}_\perp)^2(\hat{\boldsymbol{h}}\cdot\boldsymbol{k}_\perp)}{2M_N^2M_h}h_{1T}^{\perp}H_1^{\perp}\right], \tag{30}$$

where a compact notation

$$\mathcal{F}[\omega fD]=\sum_q e_q^2\int d^2\boldsymbol{p}_\perp d^2\boldsymbol{k}_\perp\delta^2(\boldsymbol{p}_\perp-\boldsymbol{k}_\perp-\boldsymbol{P}_{h\perp}/z)\omega(\boldsymbol{p}_\perp,\boldsymbol{k}_\perp)f^q(x,\boldsymbol{p}_\perp^2)D^q(z,z^2\boldsymbol{k}_\perp^2) \tag{31}$$

is used. Then we obtain the $\sin(3\phi_h-\phi_S)$ asymmetry

$$A_{UT}^{\sin(3\phi_h-\phi_S)}=\frac{\frac{2\alpha^2}{sxy^2}(1-y)F_{UT}^{\sin(3\phi_h-\phi_S)}}{\frac{2\alpha^2}{sxy^2}(1-y+\frac{1}{2}y^2)F_{UU}}. \tag{32}$$

First, we will present the results for the ratio of (the first moment of) pretzelosity (i.e. $L^q(x)$ equivalently) and unpolarized distributions, in both approaches. As we mentioned above, we can only calculate valence quarks distributions in approach 1, whereas in approach 2 we can take into account the sea quark contribution in $f_1(x)$. For approach 1, we can use Eqs. (19)–(21) directly to calculate. For approach 2, we adopt the CTEQ6L parametrization [20] for the unpolarized distribution in this paper and assume a Gaussian form factor of transverse momentum as suggested in Ref. [25]:

$$f_1(x,\boldsymbol{p}_\perp)=f_1(x)\frac{\exp(-p_\perp^2/p_{av}^2)}{\pi p_{av}^2}, \tag{33}$$

with $p_{av}^2=0.25\ \text{GeV}^2$.

Results are shown in Fig. 1, with a fixed angle $\theta = \pi/4$ and an input scale at $Q^2 = 4$ GeV^2. At first sight it seems strange that the ratio of pretzelosity versus unpolarized distribution is small in approach 1 compared to that in approach 2, as there is no sea contribution in the denominator of approach 1. We can make a brief analysis by taking d quark as an example and we could ignore sea quarks for simplicity first. In approach 1, we have

$$\begin{aligned} \mathrm{I} = \frac{h_{1T}^{\perp(dv)}(x)}{f_1^{dv}(x)} &= \frac{1}{3}\frac{\int d^2\boldsymbol{p}_\perp \varphi_V^2(x, p_\perp^2) W_V(x, p_\perp^2)}{\int d^2\boldsymbol{p}_\perp \varphi_V^2(x, p_\perp^2)} \\ &= \frac{1}{3}\frac{\int d^2\boldsymbol{p}_\perp \exp\{-\frac{1}{4\alpha_D^2}[\frac{m_q^2+p_\perp^2}{x} + \frac{m_D^2+p_\perp^2}{1-x}]\} W_V(x, p_\perp^2)}{\int d^2\boldsymbol{p}_\perp \exp\{-\frac{1}{4\alpha_D^2}[\frac{m_q^2+p_\perp^2}{x} + \frac{m_D^2+p_\perp^2}{1-x}]\}} \\ &= \frac{1}{3}\int dt e^{-t} W_V(x, 4\alpha_D^2 x(1-x)t), \qquad \left(t = \frac{p_\perp^2}{4\alpha_D^2 x(1-x)}\right). \end{aligned} \tag{34}$$

In approach 2, we have

$$\begin{aligned} \mathrm{II} = \frac{h_{1T}^{\perp(dv)}(x)}{f_1^{dv}(x)} &= \frac{1}{3}\frac{\int d^2\boldsymbol{p}_\perp d_v^{\mathrm{cteq}}(x, p_\perp^2) W_V(x, p_\perp^2)}{\int d^2\boldsymbol{p}_\perp d_v^{\mathrm{cteq}}(x, p_\perp^2)} \\ &= \frac{1}{3}\int d^2\boldsymbol{p}_\perp \frac{\exp(-p_\perp^2/p_{av}^2)}{\pi p_{av}^2} W_V(x, p_\perp^2) \\ &= \frac{1}{3}\int dt e^{-t} W_V(x, p_{av}^2 t), \qquad \left(t = \frac{p_\perp^2}{p_{av}^2}\right). \end{aligned} \tag{35}$$

We can easily prove that $W_D(x, p_\perp^2)$ is an increasing function of $p_\perp^2$ and usng the inequality

$$\begin{aligned} &4\alpha_D^2 x(1-x) \le \alpha_D^2 < p_{av}^2, \\ &(\alpha_D = 330 \text{ MeV}, p_{av} = 500 \text{ MeV}) \end{aligned} \tag{36}$$

we get that I < II, which means that two ratios can be quite different due to different parametrizations. Even if we consider the sea quarks in the denominator, II will be suppressed, but still can be larger than I. A similar analysis can be applied to the u quark though it is a little more complicated, and we can argue that it is possible that II is larger than I. From the above analysis we find the different transverse momentum dependence of quark distribution functions may cause a big difference in model predictions. This suggests the necessity to include transverse momentum dependence in data analysis. Despite the differences, both approaches give the prediction that the ratio $h_{1T}^{\perp(1)qv}(x)/f_1^q(x)$ is small, which indicates that the relativistic effect, or the quark orbital angular momentum as we suggested in our paper, is not significant, if we will integrate the transverse momentum in data analysis.

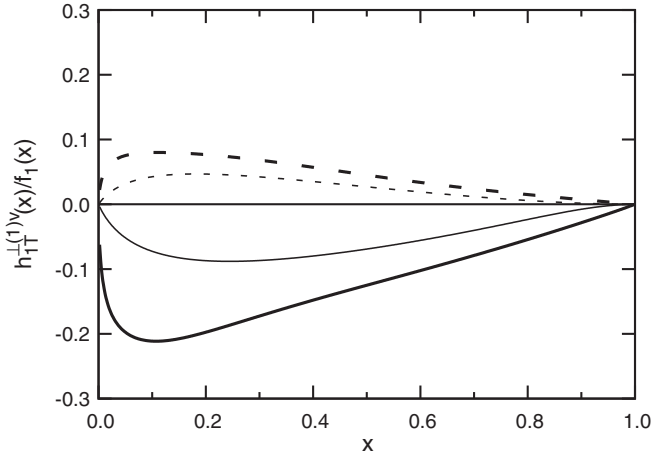

FIG. 1. The ratio $h_{1T}^{\perp(1)qv}(x)/f_1^q(x)$. Solid curves for the u quark and dashed curves for the d quark. Thin curves correspond to approach 1, while thick curves correspond to approach 2.

Before calculating the asymmetry, we still have to know the form for fragmentation functions. For the ordinary fragmentation function, we also adopt the Gaussian ansatz suggested in Ref. [25]

$$D_1(z, z^2\boldsymbol{k}_\perp^2) = D_1(z)\frac{\exp(-z^2k_\perp^2/R^2)}{\pi R^2}, \tag{37}$$

with $R^2 = 0.2$ GeV^2, and the parametrization for $D_1(z)$ can be found in Ref. [26]. The Collins function we use in this paper was also given by Anselmino *et al.* [27], which is also a Gaussian function in fact.

Next, we will present the numerical results of $\sin(3\phi_h - \phi_S)$ asymmetry in the SIDIS at different kinematics. For HERMES experiments, only the result on the proton target is calculated, while for COMPASS experiments, the proton, deuteron, and neutron targets are all assumed. As to Jefferson Lab (JLab) experiments, the result on the proton and neutron[1] targets are presented. The kinematics are shown in Table II.

The results are shown in Figs. 2–4. Obviously, different approaches to distribution functions give quite different predictions, and this can be understood from Fig. 1. Similarly, when we calculate the asymmetry, only valence quarks are summed over in approach 1, whereas in approach 2, all the flavors are summed over including the sea

[1]In fact, a ^{3}He target is used to extract neutron data in JLab experiments.

TABLE II. Kinematics at HERMES, COMPASS, and JLab.

HERMES	COMPASS	JLab
$p_{\rm lab} = 27.6$ GeV	$p_{\rm lab} = 160$ GeV	$p_{\rm lab} = 12$ GeV
$Q^2 > 1$ GeV^2	$Q^2 > 1$ GeV^2	$Q^2 > 1$ GeV^2
$W^2 > 10$ GeV^2	$W^2 > 25$ GeV^2	$W^2 > 4$ GeV^2
$0.023 < x < 0.4$		$0.1 < x < 0.6$
$0.1 < y < 0.85$	$0.1 < y < 0.9$	$0.4 < y < 0.85$
$0.2 < z < 0.7$	$0.2 < z < 1$	$0.4 < z < 0.7$

quarks in the denominator. Perhaps approach 2 might be closer to the realistic situation, because the parametrization has been well constrained by many experiments and can fit the current data much better than a simple model calculation.

Besides the difference, the two approaches also have something in common. First, we find that both approaches predict that the asymmetries are of different sign for π^+ and π^- productions. Second, we notice that the asymmetry decreases as x increases in the valence region, which is quite different from some other known effects, e.g., the $\sin(\phi_h + \phi_S)$ and $\sin(\phi_h - \phi_S)$ asymmetries. This can be explained by the ratio of the pretzelosity and unpolarized distribution shown in Fig. 1. Another important feature that might be concerned by experiments is that the asymmetry is small, up to a maximum less than 1%. Here taking approach 2 as an example, we could make a comparison of our result with transversity and corresponding $\sin(\phi_h + \phi_S)$ asymmetry, which have been intensively studied in recent years. These two asymmetries can be simply written as

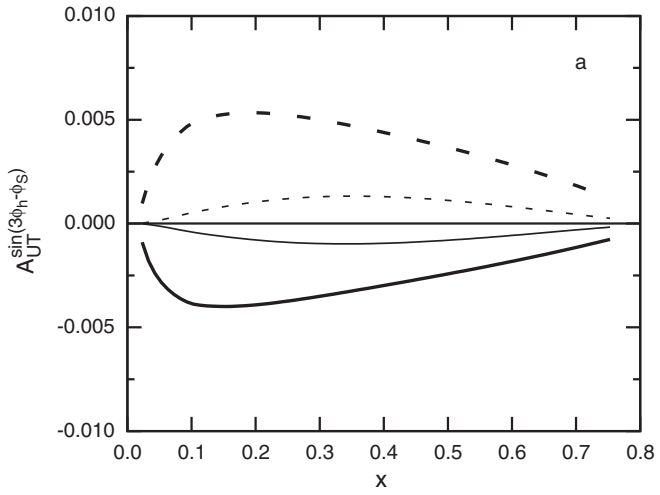

FIG. 2. $\sin(3\phi_h - \phi_S)$ asymmetry as a function of x at HERMES kinematics. Solid curves for the π^+ production and dashed curves for the π^- production. Thin curves correspond to approach 1, while thick curves correspond to approach 2. Only the proton target is assumed here.

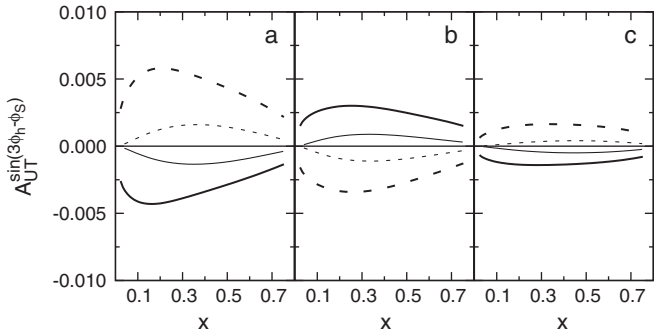

FIG. 3. Same as Fig. 2, but at COMPASS kinematics. A for proton target, B for neutron target, and C for deuteron target.

$$A_{UT}^{\sin(3\phi_h-\phi_S)} \sim \frac{\omega_1 h_{1T}^{\perp(1)} H_1^{\perp(1/2)}}{f_1 D_1},$$
$$A_{UT}^{\sin(\phi_h+\phi_S)} \sim \frac{\omega_2 h_1 H_1^{\perp(1/2)}}{f_1 D_1}. \quad (38)$$

The ratio for $h_{1T}^{\perp(1)}/f_1$ has been shown in Fig. 1, and that for h_1/f_1 can be found in Ref. [28]. We can clearly find that compared with transversity, (the first moment of) pretzelosity is suppressed by 1/2–1/10. As to the oscillation function $\omega(\boldsymbol{p}_\perp, \boldsymbol{k}_\perp)$, we could also make an estimation on its effect by integrating the angle dependence of the two vectors $\boldsymbol{p}_\perp$ and $\boldsymbol{k}_\perp$ first,

$$\frac{\tilde{\omega}_1}{\tilde{\omega}_2} \sim \frac{\int d\phi_p d\phi_k |P_{h\perp}|^3 \omega_1(\boldsymbol{p}_\perp, \boldsymbol{k}_\perp)}{\int d\phi_p d\phi_k |P_{h\perp}|^3 \omega_2(\boldsymbol{p}_\perp, \boldsymbol{k}_\perp)} = \frac{3p_\perp^2}{2p_\perp^2 + k_\perp^2}, \quad (39)$$

where we multiply ω by a weight $|P_{h\perp}|^3$ just for simplifying the estimation. For a rough estimation, we assume $\langle p_\perp^2 \rangle \approx p_{av}^2 = 0.25$ GeV^2, $\langle k_\perp^2 \rangle \approx R^2/\langle z \rangle^2 = 0.25/\langle z \rangle^2$ GeV^2, where $\langle z \rangle = 0.36$ in HERMES. We find that the ratio is about $0.3 \sim 0.4$. So from the above analysis, the $\sin(3\phi_h - \phi_S)$ asymmetry is suppressed by an order or more compared with the $\sin(\phi_h + \phi_S)$ asymmetry. According to the HERMES data [29], the size of $\sin(\phi_h + \phi_S)$ asymmetry is about a few percent, so our result for a small $\sin(3\phi_h - \phi_S)$ asymmetry is reasonable

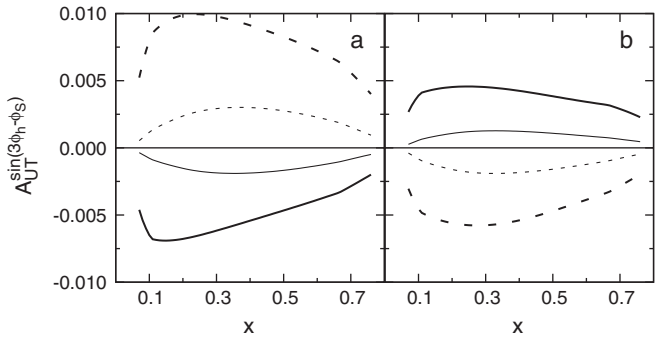

FIG. 4. Same as Fig. 2, but at JLab kinematics. A for proton target and B for neutron target.

from the above expectation. Such small asymmetry seems to be consistent with the preliminary COMPASS data [30], thus it would be a challenge for further experiments to measure pretzelosity without transverse momentum information.

However, the inclusion of transverse momentum dependence in data analysis may provide a viable way to extract pretzelosity from $\sin(3\phi_h - \phi_S)$ asymmetry measurements. We observe that both the Melosh-Wigner rotation factor for $h_{1T}^{\perp(1)}$ and the ratio as Eq. (39) shows are increasing functions of $p_\perp^2$, which enlightens us that selecting large $p_\perp$ events in data analysis might enhance the asymmetry. Unfortunately, the intrinsic parton momentum $p_\perp$ cannot be directly manipulated during the measurements. A compromise method is to select large $P_{h\perp}$ events instead, for $P_{h\perp}$ can be directly measured. In this prescription, we can exclude most small $p_\perp$ events and ensure that most large $p_\perp$ events will come into data analysis. Next we will recalculate our results with a cutoff $P_{h\perp} > 1.0$ GeV, meanwhile, we will investigate the $P_{h\perp}$ dependence of the asymmetry. The results are shown in Figs. 5–7. As we expect, the x dependence of the asymmetry is indeed enhanced by a few times, thus it might be measurable for the experiments, though high statistics would be required due to the cutoff. The $P_{h\perp}$ dependence of the asymmetry is also presented, and it can reach as large as several percent, so it provides an auxiliary measurable quantity to extract pretzelosity. Although our proposal to consider to cut off the small $P_{h\perp}$ events will enhance the asymmetry, we should be aware about this disposal. Our calculation is a leading order approximation and based on the factorization for the SIDIS, but the factorization was proved to be valid only in the region $\Lambda_{\rm QCD} \ll P_{h\perp} \ll Q$ [31]. The ideal kinematic regime to study transverse momentum dependent parton distributions is $P_{h\perp} \sim \Lambda_{\rm QCD}$ and not too large Q^2. Otherwise, the gluon radiation will be important, and a higher order pQCD correction will contribute. As pointed out in Ref. [32], this transition point is around $P_{h\perp} \approx$

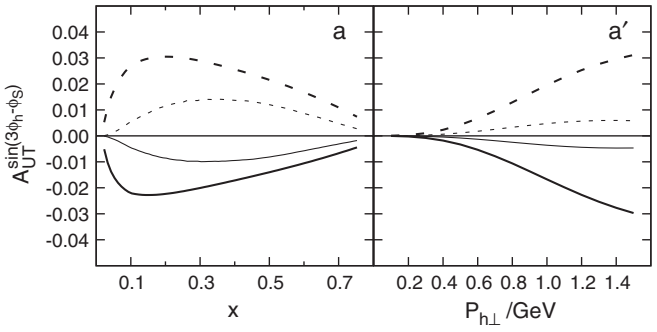

FIG. 5. The left panel shows the x dependence of the asymmetry with a cutoff $P_{h\perp} > 1.0$ GeV, while the right panel shows the $P_{h\perp}$ dependence of the asymmetry after integrating all the other kinematic variables. The curves used here are the same as that in Fig. 2.

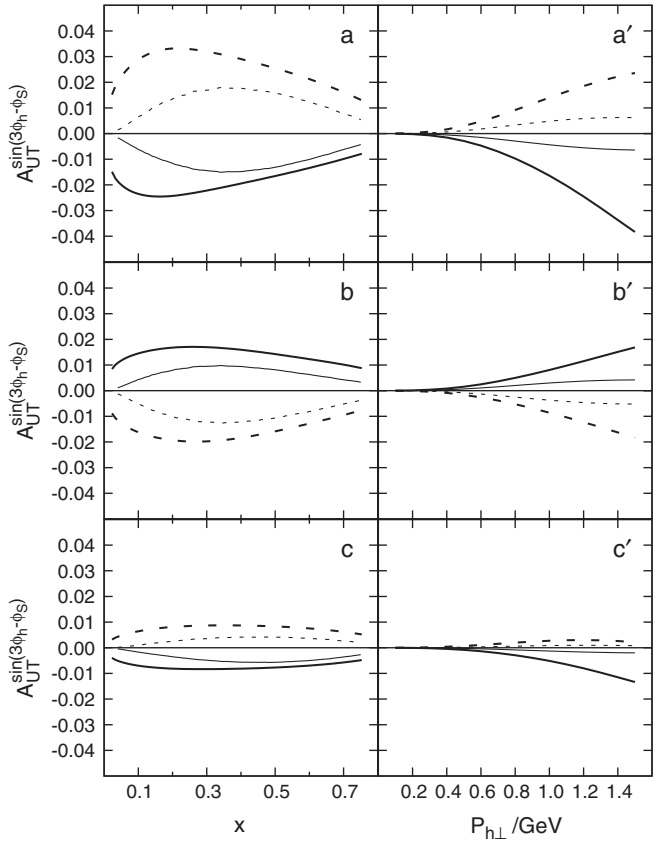

FIG. 6. Same as Fig. 5, but at COMPASS kinematics. The upper, middle, and lower panels correspond to the proton, neutron, and deuteron target, respectively.

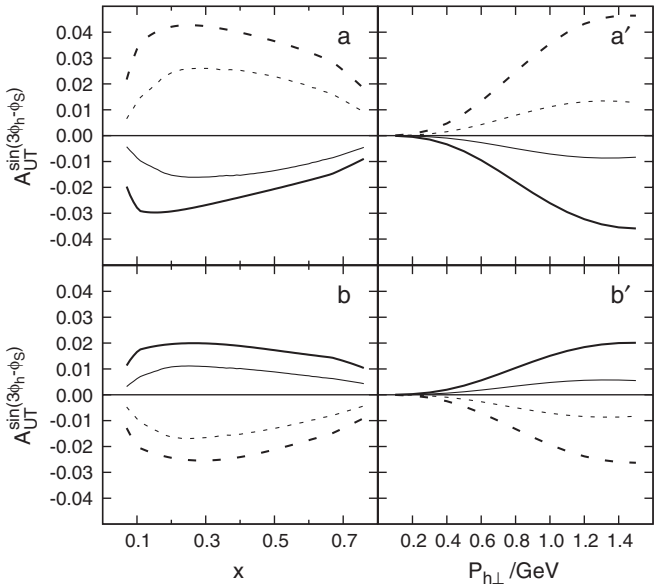

FIG. 7. Same as Fig. 5, but at JLab kinematics. The upper and lower panels correspond to the proton and neutron target, respectively.

1 GeV, and the parameters such as the Gaussian widths we used are suitable at $P_{h\perp} \leq 1$ GeV. So we must be careful about our extension analysis to a larger $P_{h\perp}$, and here we assume that our results at a little larger $P_{h\perp}$ but not too larger than 1 GeV, are still acceptable. For the experiments, they can choose an appropriate cutoff for convenience, and meanwhile we suggest an upper limit smaller than 2 GeV for $P_{h\perp}$. Another problem is that the events will be strongly suppressed at $P_{h\perp} \gg \Lambda_{\rm QCD}$, so it is a challenge for the experiments to collect more data. Anyway, we expect further experiments will bring us more information about it.

VI. SUMMARY

How to separate the nucleon spin into the intrinsic spin and orbital angular momentum parts of the constituents is a fundamental but difficult task. We have shown some debates on defining the quark orbital angular momentum in the beginning of our paper and pointed out that each definition has its advantage and disadvantage. However, disregarding the rationality of the theoretical definition, we can obtain the quark orbital angular momentum under each definition, although they might not be the real desired quantity. In Ref. [7], where the expression $\psi^{\dagger}\vec{x} \times (-i\nabla)\psi$ was used as the definition, a quantity $L(x)$ representing the quark orbital angular momentum in the light-cone gauge was obtained. In this paper, also working in the light-cone representation, we found that $L(x)$ has a simple relation with the so-called pretzelosity distribution.

Pretzelosity is one of the eight leading twist TMD functions, whose feature has been discussed in Ref. [8]. It is known that pretzelosity is considered as the difference between the helicity and transversity distributions, reflecting the relativistic effect of the spin structure. But according to Ref. [7], the moment of pretzelosity is nothing but the quark orbital angular momentum. So it provides a new possibility to access the quark orbital angular momentum through pretzelosity, and fortunately, pretzelosity can be measured in the SIDIS through $\sin(3\phi_h - \phi_S)$ asymmetry. In our paper, under the framework of the SU(6) quark-diquark model, we use two approaches to calculate pretzelosity, and we present our numerical prediction on the $\sin(3\phi_h - \phi_S)$ asymmetry under three kinematics for HERMES, COMPASS, and JLab experiments. If we do not apply any extra constrained condition, our prediction shows a small asymmetry that might bring a great challenge for experiments. However, after applying a cutoff on $P_{h\perp}$, we get an enhanced asymmetry which is measurable for experiments, though we should still be careful that $P_{h\perp}$ must not be too large. We expect that future measurements can bring us exciting new insights on the spin of the nucleon by including information of transverse momentum dependence in data analysis.

ACKNOWLEDGMENTS

We are grateful to Harut Avakian, Wen Qian, Jacques Soffer, and Feng Yuan for useful discussions. This work is partially supported by National Natural Science Foundation of China (Nos. 10721063, 10575003, 10528510), by the Key Grant Project of Chinese Ministry of Education (No. 305001), by the Research Fund for the Doctoral Program of Higher Education (China).

[1] P. G. Ratcliffe, Phys. Lett. B **192**, 180 (1987); X. Ji, J. Tang, and P. Hoodbhoy, Phys. Rev. Lett. **76**, 740 (1996); P. Hagler and A. Schäfer, Phys. Lett. B **430**, 179 (1998); A. Harindranath and R. Kundu, Phys. Rev. D **59**, 116013 (1999).

[2] S. J. Brodsky, D. S. Hwang, B. Q. Ma, and I. Schmidt, Nucl. Phys.**B593**, 311 (2001).

[3] X. Ji, Phys. Rev. Lett. **78**, 610 (1997).

[4] A. Airapetian *et al.* (HERMES Collaboration), Phys. Rev. D **75**, 011103 (2007); J. High Energy Phys. 06 (2008) 066.

[5] G. F. de Téramond and S. J. Brodsky, Phys. Rev. Lett. **102**, 081601 (2009).

[6] X. S. Chen, X. F. Lu, W. M. Sun, F. Wang, and T. Goldman, Phys. Rev. Lett. **100**, 232002 (2008).

[7] B.-Q. Ma and I. Schmidt, Phys. Rev. D **58**, 096008 (1998).

[8] H. Avakian, A. V. Efremov, P. Schweitzer, and F. Yuan, Phys. Rev. D **78**, 114024 (2008).

[9] B. Pasquini, S. Cazzaniga, and S. Boffi, Phys. Rev. D **78**, 034025 (2008).

[10] S. J. Brodsky, T. Huang, and G. P. Lepage, in *Quarks and Nuclear Forces*, edited by D. Fries and B. Zeitnitz Springer, Tracts in Modern Physics Vol. 100 (Springer, New York, 1982); S. J. Brodsky, T. Huang, and G. P. Lepage, in *Particles and Fields-2*, edited by A. Z. Capri and A. N. Kamal (Plenum, New York, 1983), p. 143.

[11] S. J. Brodsky, H.-C. Pauli, and S. S. Pinsky, Phys. Rep. **301**, 299 (1998).

[12] P. J. Mulders and R. D. Tangerman, Nucl. Phys. **B461**, 197 (1996); **B484**, 538 (1997).

[13] K. Goeke, A. Metz, and M. Schlegel, Phys. Lett. B **618**, 90 (2005).

[14] V. Barone, A. Drago, and P. G. Ratcliffe, Phys. Rep. **359**, 1 (2002).

[15] B.-Q. Ma, Phys. Lett. B **375**, 320 (1996); B.-Q. Ma, I. Schmidt, J. Soffer, and J.-J. Yang, Phys. Rev. D **62**, 114009 (2000).

[16] H. J. Melosh, Phys. Rev. D **9**, 1095 (1974); E. Wigner, Ann. Math. **40**, 149 (1939).

[17] B.-Q. Ma, J. Phys. G **17**, L53 (1991); B.-Q. Ma and Q.-R.

Zhang, Z. Phys. C **58**, 479 (1993).
[18] B.-Q. Ma, D. Qing, and I. Schmidt, Phys. Rev. C **65**, 035205 (2002).
[19] T. Huang, B.-Q. Ma, and Q.-X. Shen, Phys. Rev. D **49**, 1490 (1994).
[20] H. L. Lai *et al.*, (CTEQ Collaboration), Eur. Phys. J. C **12**, 375 (2000).
[21] I. Schmidt and J. Soffer, Phys. Lett. B **407**, 331 (1997); B.-Q. Ma, I. Schmidt, and J. Soffer, Phys. Lett. B **441**, 461 (1998).
[22] A. Bacchetta, F. Conti, and M. Radici, Phys. Rev. D **78**, 074010 (2008).
[23] A. Kotzinian, Nucl. Phys. **B441**, 234 (1995).
[24] A. Bacchetta, M. Diehl, K. Goekeb, A. Metzb, P. J. Mulders, and M. Schlegel, J. High Energy Phys. 02 (2007) 093.
[25] M. Anselmino, M. Boglione, U. DAlesio, A. Kotzinian, F. Murgia, and A. Prokudin, Phys. Rev. D **71**, 074006 (2005).
[26] S. Kretzer, E. Leader, and E. Christova, Eur. Phys. J. C **22**, 269 (2001).
[27] M. Anselmino, M. Boglione, U. DAlesio, A. Kotzinian, S. Melis, F. Murgia, A. Prokudin, and C. Türk, arXiv: 0807.0173.
[28] B.-Q. Ma, I. Schmidt, and J.-J. Yang, Phys. Rev. D **65**, 034010 (2002).
[29] A. Airapetian *et al.* (HERMES Collaboration), Phys. Rev. Lett. **94**, 012002 (2005).M. Diefenthaler (HERMES Collaboration), arXiv:0706.2242.
[30] A. Kotzinian (COMPASS collaboration), arXiv: 0705.2402.
[31] X. Ji, J.-P. Ma, and F. Yuan, Phys. Lett. B **597**, 299 (2004); X. Ji, J.-P. Ma, and F. Yuan, Phys. Rev. D**71**, 034005 (2005).
[32] M. Anselmino, M. Boglione, A. Prokudin, and C. Türk, Eur. Phys. J. A **31**, 373 (2007).